AN ACCURATE EARLY TIME SOLUTION FOR A RISING FIREBALL MODEL

Conrad L. Longmire, et al

Mission Research Corporation

Prepared for:

Advanced Research Projects Agency
Defense Nuclear Agency

October 1972

DNA 2967T
OCTOBER 1972
MRC-R-20

AN ACCURATE EARLY TIME SOLUTION FOR A RISING FIREBALL MODEL

C. Longmire
G. McCartor
N. Carron
F. Fajen

Work Supported By
ADVANCED RESEARCH PROJECTS AGENCY
Under Contract F30602-71-C-0374
(Monitored by The Rome Air Development Command)

and

DEFENSE NUCLEAR AGENCY
Under Contract DNA001-72-C-0114

Mission Research Corporation
One Presidio Avenue
Santa Barbara, California 93101

Unclassified

Security Classification

DOCUMENT CONTROL DATA - R & D

(Security classification of title, body of abstract and indexing annotation must be entered when the overall report is classified)

1. ORIGINATING ACTIVITY (Corporate author)	2a. REPORT SECURITY CLASSIFICATION
Mission Research Corporation One Presidio Avenue Santa Barbara, California 93101	Unclassified 2b. GROUP

3. REPORT TITLE

AN ACCURATE EARLY TIME SOLUTION FOR A RISING FIREBALL MODEL

4. DESCRIPTIVE NOTES (Type of report and inclusive dates)

Topical Report

5. AUTHOR(S) (First name, middle initial, last name)

Conrad L. Longmire
Gary D. McCartor
Frederic E. Fajen
Neal J. Carron

6. REPORT DATE	7a. TOTAL NO. OF PAGES	7b. NO. OF REFS
October 1972	36	5

8a. CONTRACT OR GRANT NO.	9a. ORIGINATOR'S REPORT NUMBER(S)
F30602-71-C-0374 DNA01-72-C-0114	MRC-R-20
b. PROJECT NO. NWED: XAX H	
c. Task & Subtask: C061	9b. OTHER REPORT NO(S) (Any other numbers that may be assigned this report)
d. Work Unit: 45	DNA 2967T

10. DISTRIBUTION STATEMENT

Approved for public release; distribution unlimited

11. SUPPLEMENTARY NOTES	12. SPONSORING MILITARY ACTIVITY
	Advanced Research Projects Agency AND Defense Nuclear Agency Washington, D.C.

13. ABSTRACT

An accurate solution for the inviscid rise of a hot gas cylindrical "bubble" surrounded by an initially smooth boundary is attempted by the method of time series expansion of the hydrodynamic flow field. The method is described and discussed in detail and early time results are presented.

I a

DD FORM 1 NOV 1473

Unclassified

Security Classification

KEY WORDS	LINK A		LINK B		LINK C	
	ROLE	WT	ROLE	WT	ROLE	WT
Bubble Rise						
Entrainment						
Mixing						
Inviscid Flow						

I b

Copy No. 6

DNA 2967T
PREPARED: MAY 1972
ISSUED: OCTOBER 1972
MRC-R-20

AN ACCURATE EARLY TIME SOLUTION FOR A RISING FIREBALL MODEL

This work was supported by the
DEFENSE NUCLEAR AGENCY
Under NWED subtask HC061-45

C. Longmire
G. McCartor
N. Carron
F. Fajen

Work Supported By
ADVANCED RESEARCH PROJECTS AGENCY
Under Contract F30602-71-C-0374
(Monitored by The Rome Air Development Command)

and

DEFENSE NUCLEAR AGENCY
Under Contract DNA001-72-C-0114

Mission Research Corporation
One Presidio Avenue
Santa Barbara, California 93101

IC

TABLE OF CONTENTS

LIST OF ILLUSTRATIONS

LIST OF TABLES

I. INTRODUCTION

The problem of the mixing of cold air into hot rising fireballs has been with us for many years (References 1 through 5). Experimental data on fireball altitude and average temperature versus time, coupled with theoretical analysis, clearly indicate that the outer envelope of the rising fireball must contain substantial amounts of air that was outside the original fireball and cold (Reference 6 through 10). Many photographs also show that cold air enters the fireball, in a gross way at least, by punching in from the bottom during and after formation of the torus. It is not at all clear, however, whether the cold air mixes fairly uniformly with the hot air, down to atomic scales, or remains as large lumps or lamina. But many problems involving air chemistry depend critically on the degree of mixing. It is therefore important to understand the mixing process.

If a bubble of hot gas is released in a colder and denser atmosphere, the difference in gravitational force per unit volume, inside and outside the bubble, causes the bubble to accelerate upwards. It is easy to show that the first motion of the bubble is as a rigid sphere, with uniform upward velocity inside and a dipole flow field outside. Thus vorticity (or a slip stream) initially develops at the surface of the bubble. It is also easy to see from the Bernoulli force $(-\rho\vec{V}\cdot\nabla\vec{V})$ arising from the first motion, that the second order effect is to flatten the bubble, decreasing its vertical thickness and increasing the horizontal diameter. Finally, one can convince one's self that the third order effect is to dimple in the bottom of the bubble.

About this general behavior one can ask several questions.

1. Is the slip stream Helmholtz unstable, i.e., do the minute irregularities present naturally in the initial surface grow and produce turbulence, thus "diffusing" the vorticity inward and outward from the original surface?

2. Is the top of the bubble Taylor unstable?

3. Assuming no initial irregularities are present, what is the eventual shape of the surface? Does the "jelly roll" wrap-up occur, and if so, how rapidly, and what is the velocity discontinuity across the wrapped-up boundary?

4. Does the flow outside the bubble separate, as in the Karman vortex street in flow past a rigid object?

To get at these questions, an accurate solution of the hydrodynamic equations for a smooth bubble is badly needed. Two-dimensional finite-difference computer solutions cannot be trusted because of problems of resolution and artificial viscosity connected fundamentally with the finite-difference method.

In this report we describe an attempt to find an accurate solution over some time interval by the method implied above in the second paragraph of this section, i.e., by expanding the flow field as a power series in time. On writing Euler's equation as

$$\rho \frac{\partial \vec{v}}{\partial t} - \rho \vec{g} + \vec{\nabla} p = - \rho \vec{v} \cdot \vec{\nabla} \vec{v} \qquad (1)$$

and assuming incompressibility, one sees that a power series expansion in time has the virtue of linearizing the problem: in the equation for $\vec{v}_n$ (the coefficient of t^n) the nonlinear term $\vec{v} \cdot \vec{\nabla} \vec{v}$ involves only v_m with $m < n$, which are already known. Since $\vec{\nabla} \cdot \vec{v} = 0$ from the assumption of incompresibility and $\vec{\nabla} \times \vec{v} = 0$ (except at the interface), harmonic expansion in space is also suggested. There remain the problems of locating the interface, applying boundary condition at it, solving for the expansion coefficients, and determining the convergence of the series. These problems are treated in detail in the following sections.

The method suggested here could be applied to either spheres or cylinders. In the work reported here we have chosen the cylindrical case.

Another important use for an accurate solution is in testing finite-difference computer codes. Solution of the same problem by finite-difference methods and the series expansion makes possible comparisons that may help answer the questions as to the existence and importance of spurious effects introduced into the solution by the numerical procedures. In Section V we give the results of such a comparison with the late-time fireball simulation code MICE. This work resulted in an improvement of MICE and a better understanding of the nature of the errors.

II. THE PROBLEM AND THE METHOD OF SOLUTION

We consider an infinitely long circular cylinder of fluid (fluid 1) of unit radius and density $\rho<1$ immersed in an infinite sea of fluid (fluid 2) of unit density. We assume that both fluids are inviscid and incompressible and that there is a uniform gravitational field of strength g. We initially have the fluids at rest and wish to solve for the time development.

We describe the system in polar coordinates with $\vec{r}$ measured from the center of mass of fluid 1 and $\theta = \pi$ along the direction of the gravitational field. The Euler equations then become

$$\text{a)}\quad \frac{\partial \vec{V}}{\partial t} + \vec{V}\cdot\nabla\vec{V} = -\frac{1}{\rho}\nabla P - (\ddot{H} + g)(\cos\theta\ \hat{r} - \sin\theta\ \hat{\theta}) \quad \text{(In fluid 1)}$$

$$\text{b)}\quad \frac{\partial \vec{V}}{\partial t} + \vec{V}\cdot\nabla\vec{V} = \nabla P - (\ddot{H}+g)(\cos\theta\ \hat{r} - \sin\theta\ \hat{\theta}) \quad \text{(In fluid 2)} \qquad (1)$$

$$\text{c)}\quad \nabla\cdot\vec{V} = 0 \quad \text{(In both fluids)}$$

Here H(t) is the distance the center of mass of fluid 1 has risen.

We must now specify the boundary conditions which determine our solution. To do this we first observe that the flow in each fluid must remain irrotational. This fact along with equation 1(c) allows us to define velocity potentials with the following properties

$$\begin{aligned} \nabla\phi_1 &= \vec{V}_1 \\ \nabla\phi_2 &= \vec{V}_2 \\ \nabla^2\phi_1 &= \nabla^2\phi_2 = 0 \end{aligned} \qquad (2)$$

We will seek solutions of the form

$$\begin{aligned} \phi_1 &= \sum A_n\, r^n \cos n\theta \\ \phi_2 &= -\sum \alpha_{-n}\, r^{-n} \cos n\theta + \dot{H}\, r\cos\theta \end{aligned} \qquad (3)$$

where the A_n's and α_{-n}'s are functions only of time.

We describe the interface between the two fluids by a function $F(\theta,t)$ which is the distance from the origin to the interface in the direction θ at time t. We then find that the normal to the boundary is given by

$$\hat{n} = \left(F\hat{r} - \frac{\partial F}{\partial \theta}\hat{\theta}\right)\left(F^2 + \left(\frac{\partial F}{\partial \theta}\right)^2\right)^{-1/2} \tag{4}$$

Here $\hat{r}$ and $\hat{\theta}$ are unit vectors in the r and θ directions.

We are now in a position to demand that the normal component of the flow and the pressure are continuous across the interface. Thus we set

$$\text{a)} \quad \hat{n}\cdot\vec{V}_1(F,\theta) = \hat{n}\cdot\vec{V}_2(F,\theta) \tag{5}$$

and

$$\text{b)} \quad \rho\left[\frac{\partial \phi_1(F,\phi)}{\partial t} + \frac{1}{2}(V_1(F,\theta))^2 + (\ddot{H}+g)F\cos\theta\right] =$$

$$\frac{\partial \phi_2(F,\theta)}{\partial t} + \frac{1}{2}(V_2(F,\theta))^2 + (\ddot{H}+g)F\cos\theta$$

Strictly speaking equation 5b should have an arbitrary function of time added to one side or the other, but since we use the equation only for varying θ this will not concern us and we omit it for simplicity. The condition

$$\lim_{r\to\infty} \vec{V}_2(r,\theta) = -\dot{H}(\cos\theta\ \hat{r} - \sin\theta\ \hat{\theta}) \tag{6}$$

is already assured by the form we have chosen for ϕ_2.

We need one more condition to determine r=0 as the center of mass of fluid 1. We use

$$\int_{r<F} \vec{V}_1(r,\theta)\, r\, dr\, d\theta = 0 \tag{7}$$

These relations along with the initial conditions $\vec{V}_1=\vec{V}_2=0$ and $F=1$ are sufficient to determine the solution.

We can now combine equations 5,4, and 3 to obtain the following equations, which form the basis of the method.

$$\text{a)} \quad -\sum nA_n F^n \cos n\theta - \frac{\partial F}{\partial \theta} \sum nA_n F^{n-1} \sin n\theta = -\sum n\alpha_n F^{-n} \cos n\theta$$

$$+ \frac{\partial F}{\partial \theta} \sum n\alpha_n F^{-(n+1)} \sin n\theta - \dot{H}\left(\frac{\partial F}{\partial \theta} \sin\theta + F\cos\theta\right)$$

$$\text{b)} \quad (1-\rho)\, g\, F\cos\theta - \rho\ddot{H} F\cos\theta + \sum \dot{\alpha}_n F^{-n}\cos n\theta + \rho\sum \dot{A}_n F^n \cos n\theta$$

$$= \frac{\rho}{2}\left[\left(\sum nA_n F^{n-1}\sin n\theta - \dot{H}\sin\theta\right)^2 + \frac{1}{2}\left(\sum n\alpha_n F^{-(n+1)}\cos n\theta + \dot{H}\cos\theta\right)^2\right]$$

Relation 7 becomes

$$\int_0^{\pi} \sum A_n F^n \cos(n+1)\theta \, d\theta = 0 \tag{9}$$

From similarity considerations or by time reversal invariance we must have A_n and α_n odd in t, H and F even in t. Thus we seek a solution of the form

$$H = \sum_{i=1}^{\infty} h_i t^{2i}$$

$$F = 1 + \sum_{i=1}^{\infty} f_i(\theta) t^{2i} \tag{10}$$

$$A_n = \sum_{i=1}^{\infty} a_{ni} t^{2i-1}$$

$$\alpha_n = \sum_{i=1}^{\infty} \alpha_{ni} t^{2i-1}$$

It is easy to see that we may find a solution of the form

$$\text{a)} \quad F = 1 + \sum_{i=1}^{\infty} \sum_{j=0}^{i} f_{ij}\, t^{2i} \cos j\theta$$

$$\text{b)} \quad A_n = \sum_{i=n}^{\infty} a_{ni}\, t^{2i-1} \tag{11}$$

$$\text{c)} \quad \alpha_n = \sum_{i=n}^{\infty} \alpha_{ni}\, t^{2i-1}$$

From these relations it is seen that if only those terms with time order less than N are kept only those An's and αn's with $n < \frac{N+1}{2}$ are non-zero. The expansions (3) thus terminate. In the same way expansion 11a contains no cos jθ's with j > N/2. Thus the expansions we have made in the spatial variables are all finite and need not be truncated. When the expansions 11 along with that for H are inserted into equations 8 and 9, recursion relations result which may be solved with the aid of a computer.

The problem of finding the Taylor series expansion for any function in the problem thus reduces to the algabraic one of determining the expansion coefficients in 11.

We have already chosen above the following units:

unit of length = initial radius of cylinder;
unit of density= density of exterior fluid.

with these choices, the unit of time is determined by:

$$\text{unit of time} = \sqrt{\frac{gR}{g_0}}\,.$$

Here g_0 is the actual value of the gravitational acceleration and g is the number that is inserted in Equation 1. In this report we use g = 3 in order to make the first term in the expansion of H be $H = \frac{1}{2} t^2 + \quad .$

It is easy to see that we may find a solution of the form

$$\text{a)} \quad F = 1 + \sum_{i=1}^{\infty} \sum_{j=0}^{i} f_{ij}\, t^{2i} \cos j\theta$$

$$\text{b)} \quad A_n = \sum_{i=n}^{\infty} a_{ni}\, t^{2i-1} \tag{11}$$

$$\text{c)} \quad \alpha_n = \sum_{i=n}^{\infty} \alpha_{ni}\, t^{2i-1}$$

From these relations it is seen that if only those terms with time order less than N are kept only those An's and αn's with $n < \frac{N+1}{2}$ are non-zero. The expansions (3) thus terminate. In the same way expansion 11a contains no cos jθ's with j > N/2. Thus the expansions we have made in the spatial variables are all finite and need not be truncated. When the expansions 11 along with that for H are inserted into equations 8 and 9, recursion relations result which may be solved with the aid of a computer.

The problem of finding the Taylor series expansion for any function in the problem thus reduces to the algabraic one of determining the expansion coefficients in 11.

We have already chosen above the following units:

unit of length = initial radius of cylinder;
unit of density= density of exterior fluid.

with these choices, the unit of time is determined by:

$$\text{unit of time} = \sqrt{\frac{gR}{g_0}}\,.$$

Here g_0 is the actual value of the gravitational acceleration and g is the number that is inserted in Equation 1. In this report we use g = 3 in order to make the first term in the expansion of H be $H = \frac{1}{2} t^2 +$.

Thus the density ρ as we use it is actually the ratio of the interior density to the exterior density. The solutions to problems with the same ρ but different R and g_0 are related by simple scaling; for problems with different ρ there is no simple scaling.

III. THE RESULTS FROM THE POWER SERIES

We have computed the coefficients for the Taylor series of the functions F, A, $\underline{\alpha}$, and H defined in the previous section through order 72. For this we used values $\rho=0.5$ and $g=3$.

Since we have no theoretical prediction for the radius of convergence we estimate this from the observed benavior of the coefficients. It appears that F, A, and $\underline{\alpha}$ converge to approximately $t^2=1$ while H converges to around 1.4 or 1.5. For values of the time less than this we can compute very accurate values for these functions.

The solid part of the curve in Figure 1 shows the height H obtained in this fashion plotted vs t^2. If the cylinder did not deform, the curve would be the straight line shown by the dotted line. As might be expected the deformation slows down the rate of rise.

Figure 2 shows the boundary F plotted at t=0.71 and 0.95. The curve for 0.71 deviates from the original circle by at most 4% while at 0.95 there is a pronounced deformation. This indicates that while initially there is only very slow deformation, the rate can be expected to increase greatly for later times.

For applications to physical phenomena, an important quantity is the discontinuity in the tangential component of the flow. In Figure 3 we have plotted this discontinuity as a function of θ at $t^2=0.5$. At this time the velocity of the center of mass is 0.6809. As is seen the discontinuity at some angles is more than twice this value. Such large shears probably indicate that for viscosities that spread this slip over only a small region finite different methods will not be able to represent the flow near the boundary at all. This information should also be useful in predicting the development of turbulence at early times.

In Figure 4 we show a representation of the flow field at $t^2=0.75$.

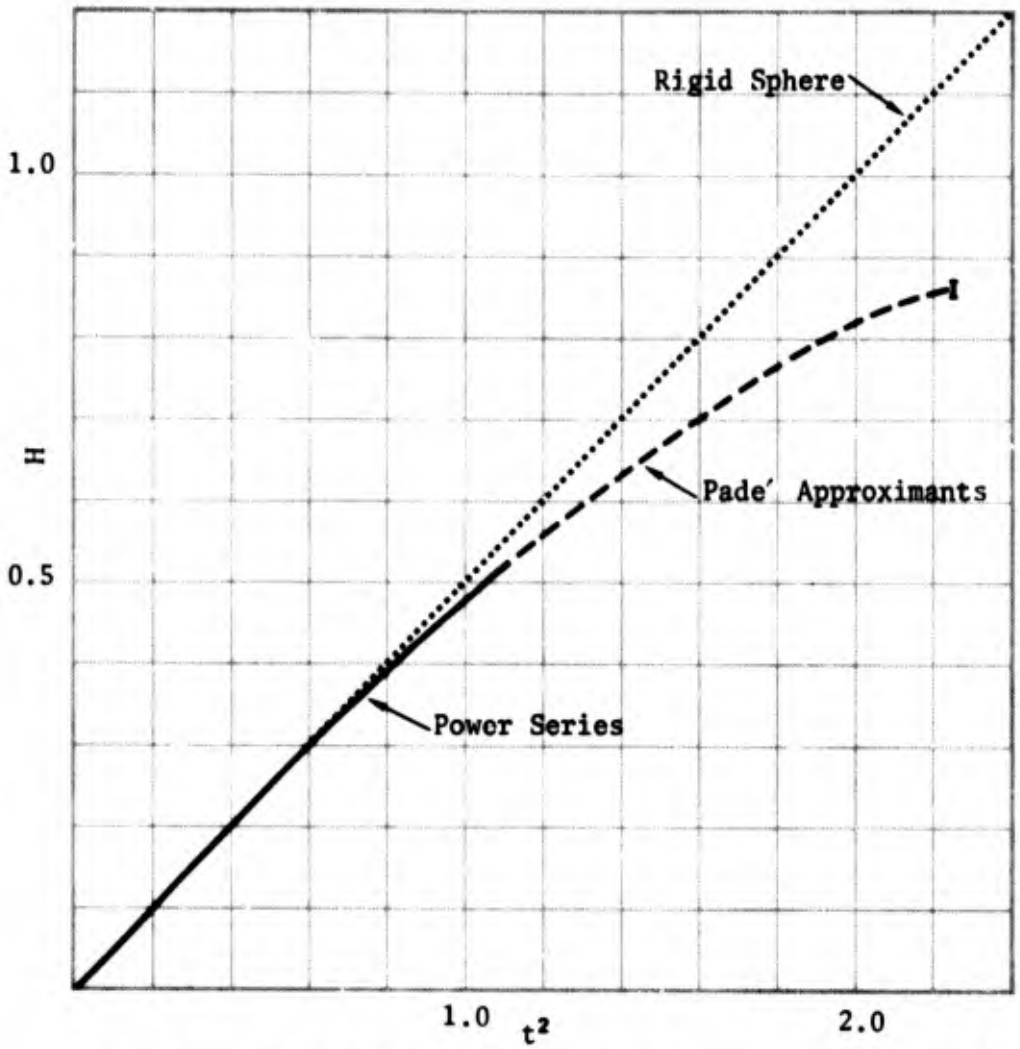

Figure 1. The height of the center of mass plotted vs. t^2.

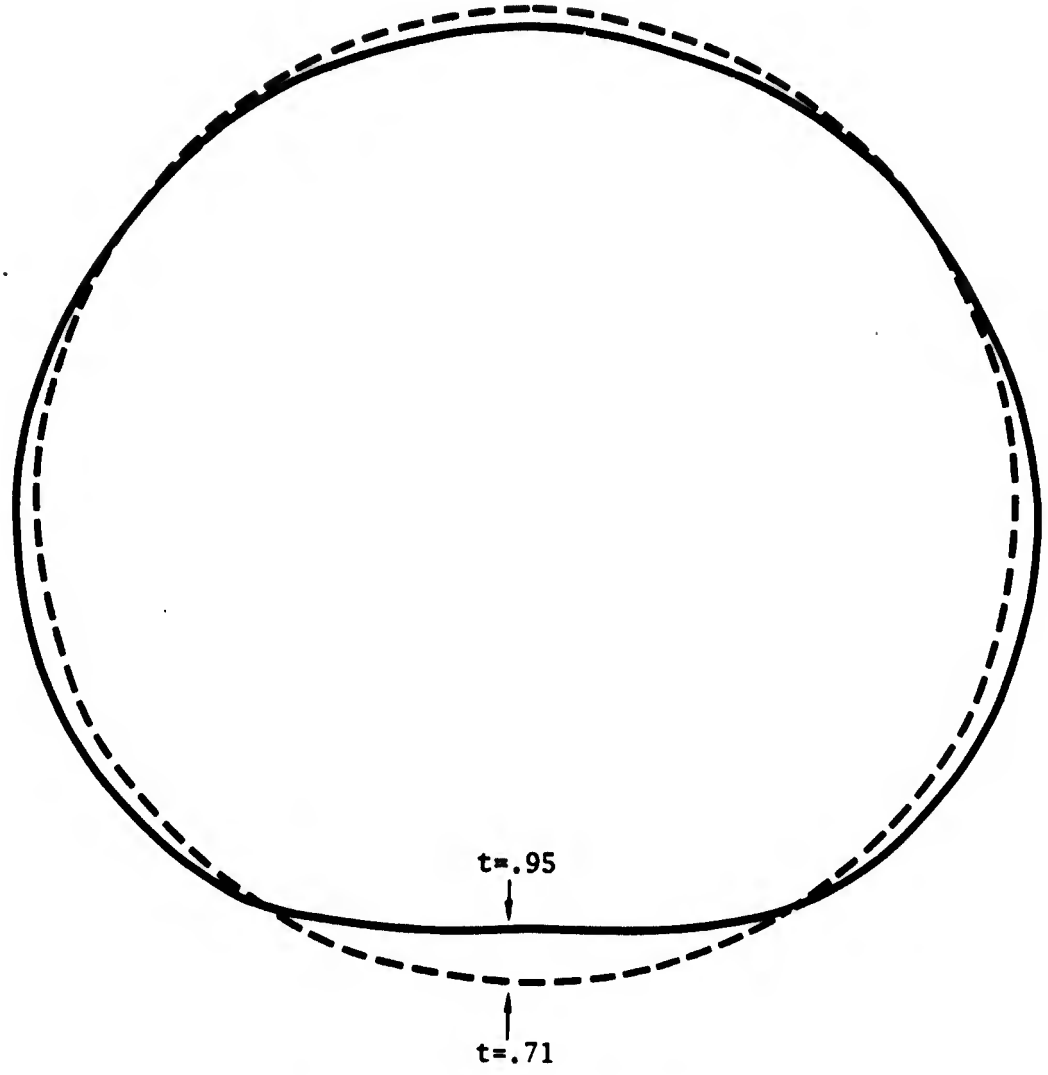

Figure 2. The boundary at t=.71 and .95.

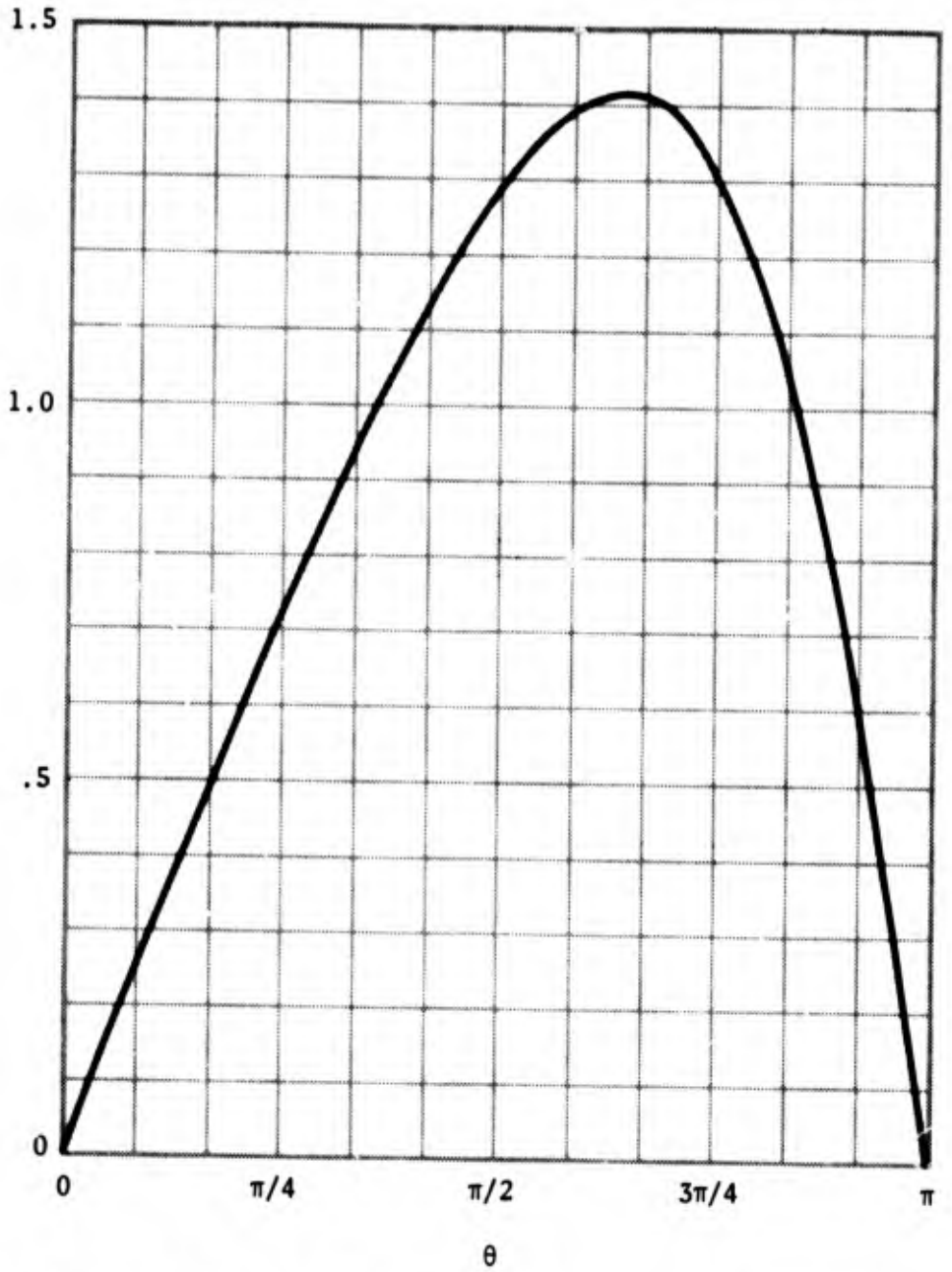

Figure 3. The discontinuity in the tangential component of the flow field plotted vs. θ at $t^2=0.75$. The velocity of the center of mass is 0.6809.

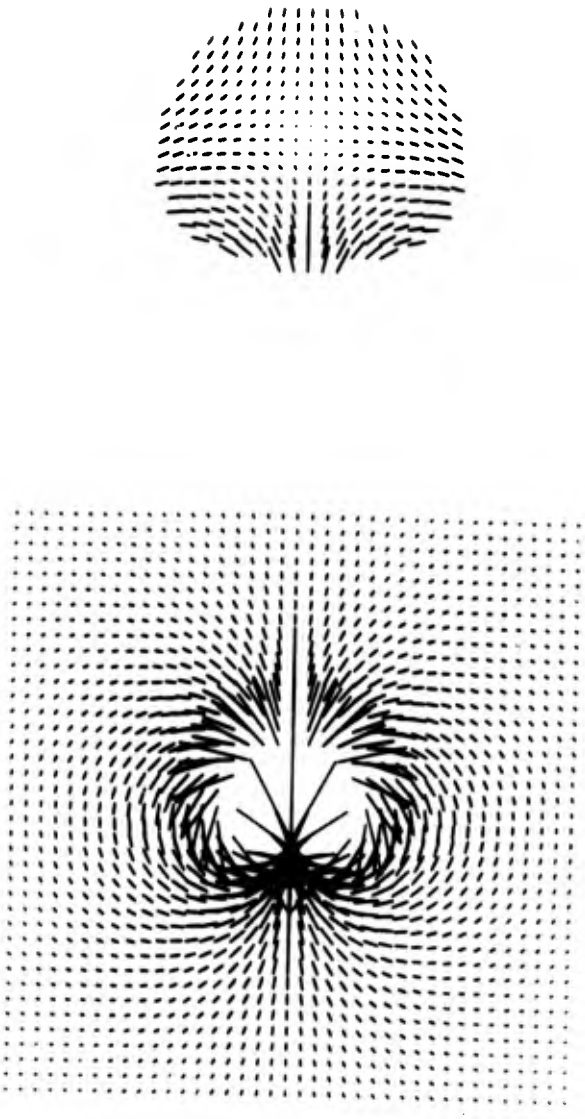

Figure 4. A graphic representation of the inside and outside flow fields at $t^2=0.75$.

IV. CONTINUATION WITH PADE´ APPROXIMANTS

While the results obtained from the power series are useful and interesting, the most important features of the problem clearly occur at times after failure of convergence of the series. To get information on this from our expansion we must sum divergent series. The best method for doing that is the method of Pade´ approximants (Reference 11).

All the coefficients hi where i is not of the for mi=2+4n are zero. Thus H has the form

$$H = t^2 H(t^4)$$

Our expansion thus gives the first 18 terms of the Taylor series for H. This allows us to form any Pade´ term [N,M] where N+M 17. (P[N,M] is a rational fraction with numerator of degree M and denominator of degree N whose Taylor series is the same as that for H through N+M+1 terms.)

Since a useful theory of the convergence of Pade´ approximants is not currently available, we must again estimate the convergence based on the appearance of the numbers. The dashed part of the curve in Figure 1 was computed in this way. The convergence is quite good until above t^2=2 where it starts to break down. At t^2=2.25 the answer is probably still good to almost two figures. To give some idea of the validity of the approximant, Table 1 gives the [N,N], [N+1,N] and [N,N+1] approximants for t^2=1.5 and 2.25.

We can also use Pade´ approximants to continue the boundary function F to later times. This is done by first doing the sum on cos(nθ) for a particular value of θ, then forming the Pade´ table for the resulting function of time.

The solid curve of Figure 5 shows the boundary at t^2=1.5 (t=1.23). It is apparent that the acceleration of the distortion suggested in the previous section is taking place. It would appear that

TABLE 1. Pade´ Approximants for H.

t^2 \ N		2	3	4	5	6	7	8
1.5	[[N+1,N]	.6713	.6700	.6707	.6703	.6702	.6704	.6704
	[N,N]	.6759	.6699	.6699	.6704	.6703	.6703	.6703
	[N,N+1]	.6708	.6700	.6706	.6703	.6705	.6703	.6703
2.25	[N+1,N]	.972	.857	.662	.856	.850	.877	.873
	[N,N]	.755	.852	.851	.885	.868	.940	.861
	[N,N+1]	.901	.856	.107	.845	.773	.942	.844

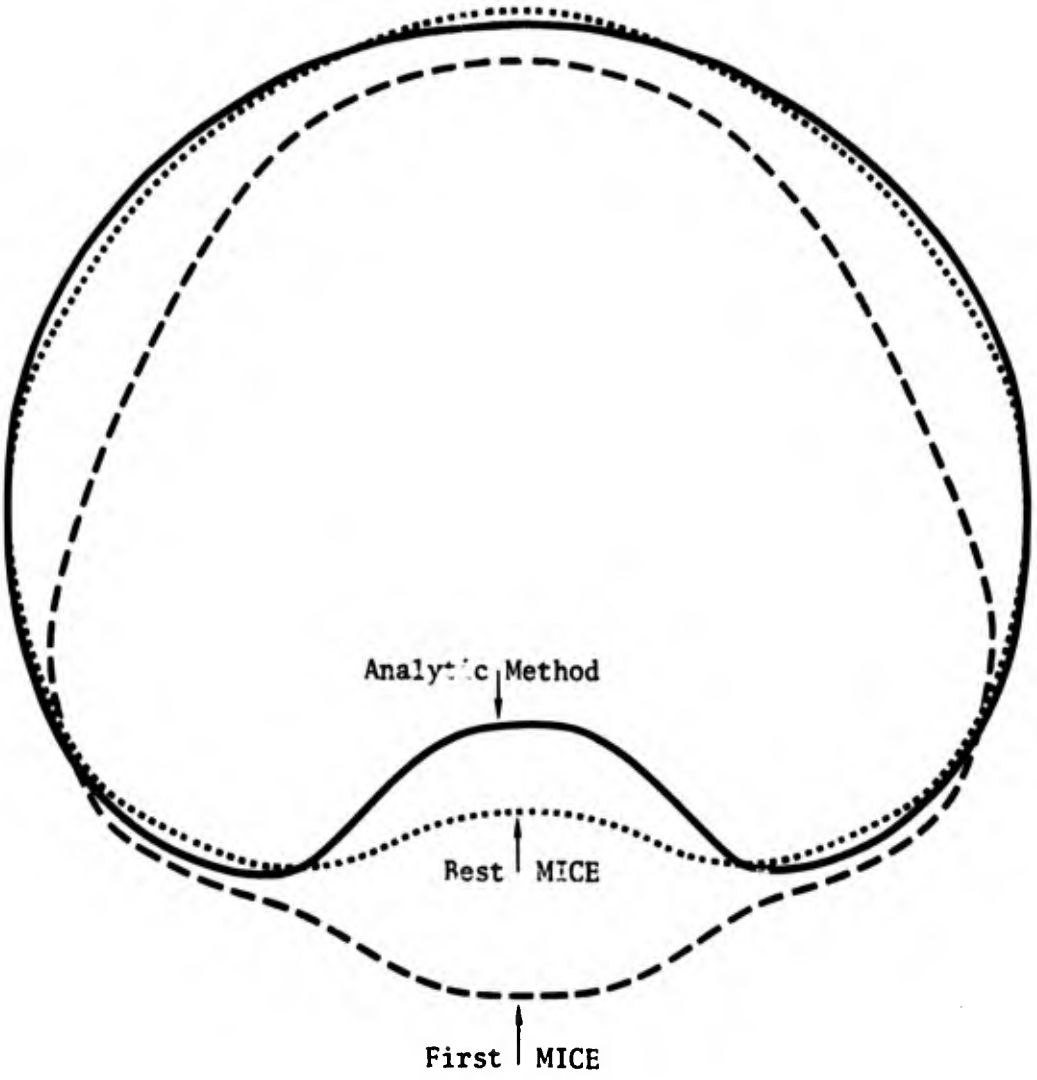

Figure 5. A comparison of the position of the boundary at $t^2 = 1.5$ as given by our method and by MICE.

the boundary has distorted more between 0.95 and 1.23 than it did between 0 and 0.95. If this continues, severe distortion or wrap up could take place a short time later.

The approximants for the upper part of the boundary ($\theta<135°$) converge for even later times than this. One can get values for these at t^2 equal to four or five. As might be expected, it is just in the interesting region where failure first occurs.

V. COMPARISON WITH MICE

We have used our results to test the finite mesh code MICE (Reference 12), which was developed to do late-time fireball simulation. Since MICE cannot do strictly incompressible flow, however, a certain amount of caution must be exercised in interpreting the results. MICE is a second order Eulerian code with variable mesh size capability. We studied a variety of mesh sizes, the smallest being one-twentieth of a radius at the center and increasing by five percent per cell in both directions. The sound speed was about ten times the maximum fluid speed.

The performance of MICE on this problem certainly improved as a result of our work. This can be seen in Figure 5 where in addition to our boundary at $t^2=1.5$ we have shown the results of an early MICE run and the final best fit we could get. During this process we learned several things, perhaps the most important being that using time-centered differencing in MICE leads to a vast improvement in accuracy. A large portion of the improvement shown in Figure 5 can be attributed to this procedure. We also found that the various diffusive processes which must be used to keep MICE stable cause substantial adverse effects. Even when these act only in the first few time steps they cause errors. It is clearly important to keep these to an absolute minimum when running this type of problem.

Even our best MICE run does not agree well in the region at the bottom. This is probably the most important region for the entrainment process. It seems to us that the finite mesh scheme will simply not allow the large gradients necessary to run this problem accurately. By going to a Lagrangian picture we could eliminate the need for diffusion, but the problem of large gradients would remain. It seems that to obtain accurate calculations for the fine details of problems like this better methods than any presently available must be developed.

It is an interesting fact that while the boundaries given by the two methods do not agree very well, the height curve given by the best MICE run is virtually indistinguishable from that of Figure 1.

VI. THE SINGULARITIES

The source of the singularities which stop the convergence of the various series of section II remains at the moment an open question. We have no theoretical understanding of why they occur or what their nature is. We can however use the Padé approximants to try to learn their positions and even perhaps a little about their type.

In Figure 6a, we have plotted the poles in the Padé approximants for H. It seems clear that the function has branch points near $1 \pm 1.6i$. This agrees with the estimated radius of convergence quite well. In Figure 6b we have plotted the poles in the approximants to $[2.5 + (1+X)^2]^{-\frac{1}{8}}$. The similarity is apparent.

The representations we have used to set up the problem can break down for several reasons. If the boundary becomes badly deformed the function F can become multivalued. If the center of mass moves to the outer fluid one would expect the representation 7 for the flow field to become invalid.

While the convergence seems to fail at times earlier than the onset of the problems mentioned above, it seems better to remove these difficulties before proceeding. We will therefore represent the boundary parametricly to allow for any expected type of distortion.

One way to do this is to define the functions $R(\phi,t)$, $\theta(\phi,t)$ which are the R,θ coordinates at time t of the particle which originally started at $\theta = \phi$. We have

$$\frac{\partial R}{\partial t} = V_r\ (R,\theta)$$

$$\frac{\partial \theta}{\partial t} = \frac{1}{R} V_\theta (R,\theta)$$

From these relations and the already computed expansion for V we can compute expansions of the form

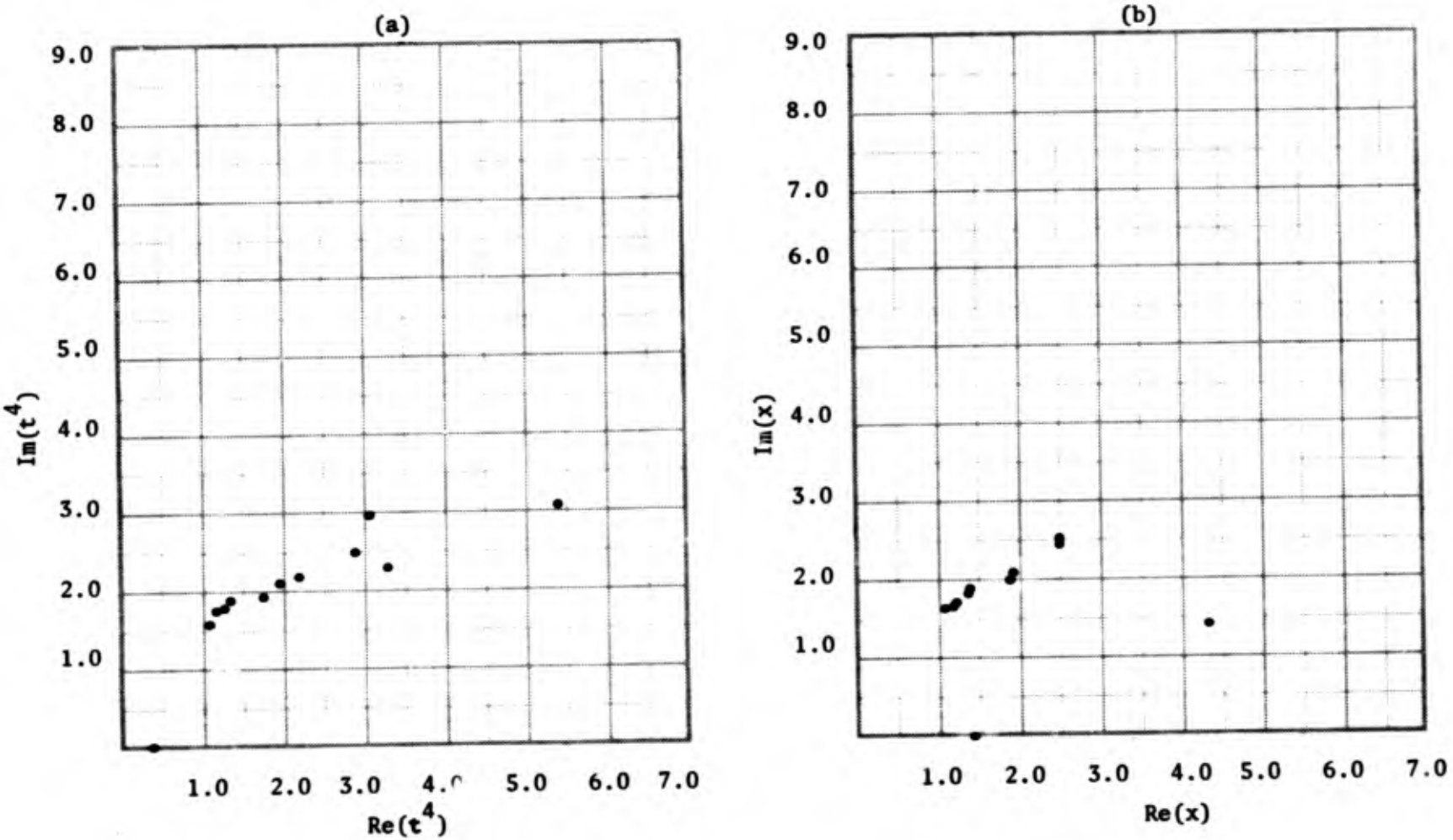

Figure 6. The poles in the Pade' approximants to the functions $H(t^4)$ and $[2.5+(1+x)^2]^{-1/8}$.

$$R(\phi,t) = 1 + \sum_{n=1}^{N} \sum_{j=0}^{n} t^{2n} d_j^n \cos j\phi$$

$$\theta(\phi,t) = \phi + \sum_{n=1}^{N} \sum_{j=1}^{n} t^{2n} e_j^n \sin j\phi$$

We can then study these with Padé approximants.

In Figure 7 we show the poles of the approximants to $\theta\left(\frac{23}{24}\pi,t\right)$ which occur in the upper right half plane. While the situation is much less clear than for H, a good guess is that there are branch points at about 1.0 ± .65i and the approximants are trying to join them with a circular cut.

The poles for the function R do not show a pattern which we have been able to interpret although very few lie near the real axis and most are scattered in the vicinity of 1.0 ± .8i.

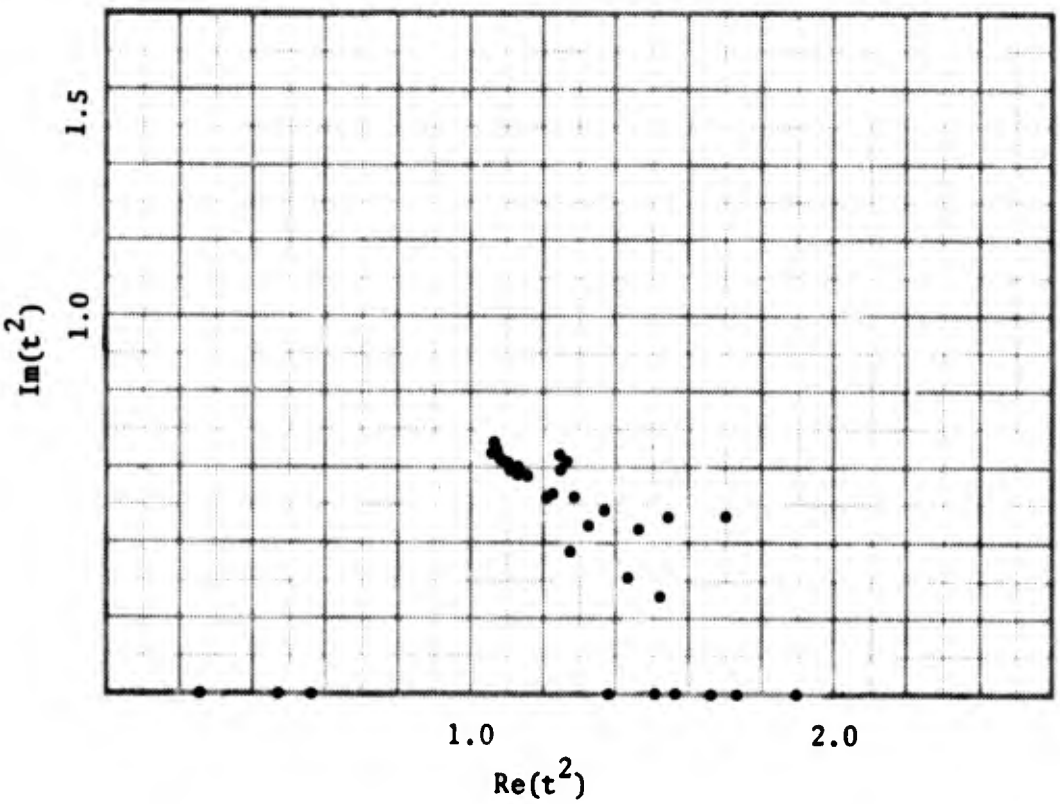

Figure 7. The poles in the Pade' approximants to the function on $\theta(23\pi/24, t^2)$.

VII. OUTLOOK

There are several ways one might attempt to extend the above work to later times. One perfectly legitimate and straightforward way is to guess. If one could guess the exact nature of the singularities one could extract them and presumably continue the remainder much further in time.

Certainly the most satisfying procedure would be to go to the original equations and derive the nature and the source of the singularities from them. The fact that the structure obviously depends not only on the dynamic equations but also on the initial and boundary conditions suggests that an integral equation formulation would be a good starting point for this. Such procedures have yielded powerful results in other fields. Any success along these lines would be more interesting and useful than that from any other method suggested here but the mathematical difficulties are not to be taken lightly.

Intermediate between these two methods is that of continuing the functions by expanding around successively later time points. For this one would expand around some point in time τ_0 then compute the flow fields and boundary at some later time τ_1. Taking these as initial conditions the equations would then be expanded about τ_1 and the process repeated.

Unfortunately for all points except the first, the spatial expansions would not terminate as they did in Section II. It would thus be necessary to truncate them keeping as many terms as computer size and speed would allow. If there are no real singularities and the truncation errors do not become large this should provide a very accurate method.

REFERENCES

1. Rohringer, G., Entrainment and Expansion Controlled Fireball Rise , DASA 1409, 1963 (U).

2. Huebsch, I. O., Development of a Water Surface Burst Fallout Model—The Rise of Atomic Clouds , USNRDL-TR-741, 1964 (U).

3. Onufriev, A., Theory of the Motion of a Vortex Ring Subjected to Gravity—Ascent of an Atomic Cloud, Prikl. Mekh. i Tekh. Fiz., No. 2, p. 3, 1967.

4. Padé, H., "Sur la représentation approchée d'une fonction pur des fractions rationnelles," Thesis, Ann. d l'Éc. Nor., (3), Vol. 9 (1892), pp. 1-93, supplement. For a report of applications to physical problems see: Baker, G. A., and J. L. Gammel, The Pade Approximant in Theoretical Physics, (Academic, New York, 1970).

5. Fajen, F. E., MICE—An Implicit Difference Scheme for MHD Calculations, DASA Report 01-71-C-054.